2024 IEEE 63rd Conference on Decision and Control (CDC)
December 16-19, 2024. MiCo, Milan, Italy

Adaptive Line-of-Sight Path Following for Curved Paths as a Maneuvering Problem

Erlend A. Basso♯, Henrik M. Schmidt-Didlaukies♯, and Kristin Y. Pettersen

***Abstract*— This paper presents the maneuvering adaptive line-of-sight (MALOS) algorithm, which guarantees global asymptotic path following and crab angle estimation for a class of underactuated vehicles in the presence of an unknown crab angle. Notably, MALOS is the first line-of-sight (LOS) guidance scheme with integral action for curved paths with truly global stability results, and not just global under the assumption that the path parameter can be selected such that the along-track error is identically zero. A case study of an autonomous underwater vehicle demonstrates the effectiveness of the MALOS algorithm.**

I. Introduction

Line-of-sight (LOS) guidance laws constitute a prominent class of methods used to generate heading reference signals for the autopilots of underactuated marine vehicles, with the ultimate goal of permitting these vehicles to follow a given path. There are two main types of LOS guidance laws, static state feedback and dynamic feedback LOS algorithms. Static state feedback LOS algorithms are known as proportional LOS guidance laws, while dynamic feedback algorithms include integral LOS (ILOS) and adaptive LOS (ALOS).

The first ILOS guidance law was introduced in [1], which assumes that the path is a straight line and places restrictions on the integral gain relative to the forward velocity. This ILOS guidance law has been experimentally verified for an uncrewed semi-submersible vehicle and an autonomous underwater vehicle (AUV) in [2], and for an underwater snake robot in [3]. The work in [4] presents the adaptive ILOS (AILOS) guidance law, which is an ILOS algorithm for which the integral state differential equation is structurally different than the classical ILOS algorithm in [1].

The extended-state-observer LOS (ELOS) guidance law was proposed in [5]. By assuming that the crab angle is small, the authors prove input-to-state stability (ISS) for the closed-loop system with respect to the crab angle estimation error. However, when the crab angle is constant, global asymptotic path following is not proven. Furthermore, the desired heading produced by the guidance law is defined implicitly, because it depends on quantities that themselves depend on the desired heading. It is not shown that this implicit relation involving the desired heading always has a well-defined and unique solution. For implementation, an explicit relation for the desired heading is constructed by replacing some instances of the current value of the desired heading in the implicit relation with the one from the previous time step.

The adaptive LOS (ALOS) guidance law was introduced in [6], where the integral state now represents an estimate of the crab angle directly. However, the approach can exhibit unwinding due to the integral state being unbounded. This problem is addressed in [7], where a locally Lipschitz projection operator is employed to ensure boundedness of the crab angle estimate. Semi-global stabilization is proven; however, no relationship between the region of attraction and the control gains or system parameters are given. More recently, ISS with respect to a function of the vehicle velocities was shown in [8]. This work does not assume that the crab angle is small, and includes a global asymptotic path following result when the crab angle is constant.

The maneuvering problem was introduced in [9] and generalized in [10] and [11]. The maneuvering problem is comprised of a geometric task, which is to ensure that the position of the vehicle converges to a desired path; and a dynamic task, which is to ensure that the path speed converges to a desired speed assignment. Proportional LOS guidance was solved as a maneuvering problem in [11] and [12], which we refer to as maneuvering LOS (MLOS). To the authors' best knowledge, there are no works in the literature where LOS algorithms with integral action are utilized to solve the maneuvering problem.

All of the non-maneuvering approaches to static and dynamic feedback LOS guidance assume that the path parameter can be chosen such that the along-track error is zero for all time. While this is a reasonable assumption for straight lines, it is not as straightforward for curved paths. In particular, a regular evolution of the path parameter can only be guaranteed for curved paths if the vehicle remains sufficiently close to the path. In other words, these approaches result in local guidance laws for curved paths.

The main contribution of this paper is the maneuvering adaptive line-of-sight (MALOS) guidance scheme. The MALOS algorithm generalizes the MLOS algorithm to the case of nonzero crab angles by including integral action in the form of crab angle parameter estimation and is the first LOS guidance scheme with integral action that solves the maneuvering problem. In particular, we modify the crab angle adaptation from the ALOS guidance law presented in [6] and synthesize a novel update law for the path parameter utilizing Lyapunov techniques. Then, we prove that the MALOS guidance law guarantees global asymptotic path following and crab angle estimation under the assumptions that the crab angle is con-

This project has received funding from the European Research Council (ERC) under the European Union's Horizon 2020 research and innovation programme, through the ERC Advanced Grant 101017697-CRÈME. The work is also supported by the Research Council of Norway through the Centres of Excellence funding scheme, project No. 223254 – NTNU AMOS.

♯ E. A. Basso and H. M Schmidt-Didlaukies contributed equally to this work and should be considered co-first authors

The authors are with the Department of Engineering Cybernetics, Norwegian University of Science and Technology, NO-7491 Trondheim, Norway {erlend.a.basso,henrik.schmidt,kristin.y.pettersen}@ntnu.no

stant and that the path has bounded curvature. Importantly, we do not assume that the crab angle is small. We remark that MALOS is truly global, and not just global provided that the path parameter can be selected such that the along-track error vanishes at all times, as is typically assumed in the analysis of LOS guidance laws. As in [8], the crab angle adaptation involves a projection operator which ensures that the crab angle estimate is bounded. However, the MALOS algorithm is structurally different from the ILOS approach in [8] in the sense that we estimate the crab angle directly. The crab angle estimate is then employed to rotate the LOS vector, while an ILOS approach such as [8] includes integral action directly into the LOS vector, instead of estimating the crab angle.

This paper is organized as follows. Section II introduces the kinematic model and some notions related to paths before Section III introduces the MLOS algorithm for curved paths defined in [11]. The main results of the paper are presented in Section IV, where the MALOS guidance law is defined and UGAS of the origin of the resulting closed-loop system is proven. Section V presents a case study where the MALOS algorithm is applied for horizontal position control of an AUV. Finally, Section VI concludes the paper.

Notation

The Euclidean norm is denoted $|x| = (x^\mathsf{T} x)^{1/2}$, and $|x|_\mathcal{A} = \inf_{y \in \mathcal{A}} |x - y|$ is the distance from x to a set $\mathcal{A} \subset \mathbb{R}^n$. The standard basis vectors in $\mathbb{R}^n$ are denoted $e_1, \ldots, e_n$. The unit circle is defined by $\mathbb{S} := \{x \in \mathbb{R}^2 : |x| = 1\}$, and the group of planar rotations by $\mathrm{SO}(2) := \{R \in \mathbb{R}^{2\times 2} : R^\mathsf{T} R = I, \det R = 1\}$. A unit vector $z \in \mathbb{S}$ maps to a rotation matrix through the map $R : \mathbb{S} \to \mathrm{SO}(2)$ defined by $R(z) := \begin{pmatrix} z & Sz \end{pmatrix}$, where $S := \left(\begin{smallmatrix} 0 & -1 \\ 1 & 0 \end{smallmatrix}\right)$. Furthermore, a function $V : X \to \mathbb{R}$, where $X \subset \mathbb{R}^n$, is proper if the preimage of any compact set $K \subset \mathbb{R}$ under V is compact. A mapping $f : X \to \mathbb{R}^m$ is said to be $\mathcal{C}^r$ if it is r-times continuously differentiable. Lastly, $\operatorname{atan2} : \mathbb{R}^2 \setminus \{0\} \to (-\pi, \pi]$ denotes the four-quadrant inverse of $\tan$.

II. Modeling

Let $p \in \mathbb{R}^2$ denote the north and east positions of a marine vehicle. The kinematic differential equation is given by

$$\dot{p} = UR(\beta)z, \tag{1}$$

where $z \in \mathbb{S}$ is considered a control input and represents the orientation (or heading) of the marine vehicle. Moreover, $U \in \mathbb{R}$ denotes the speed over ground and $\beta = (\beta_1, \beta_2) \in \mathbb{S}$ is the crab vector, respectively. These quantities can be defined in terms of the surge and sway velocities $u = (u_1, u_2) \in \mathbb{R}^2$ by

$$U := |u|, \tag{2}$$

$$\beta := \frac{1}{|u|} u. \tag{3}$$

The crab angle $\beta_c \in (-\pi, \pi]$ and the crab vector $\beta \in \mathbb{S}$ are related by

$$\beta_c := \operatorname{atan2}(\beta_2, \beta_1), \tag{4}$$

$$\beta = \begin{pmatrix} \cos\beta_c \\ \sin\beta_c \end{pmatrix}. \tag{5}$$

We remark that (1) reduces to a unicycle model if the crab angle is zero, i.e. $R(\beta) = I$. A unicycle model is often used to model a marine vehicle in transit, see e.g. [12], [13].

Assumption 1. *The speed over ground U is constant and satisfies $U > 0$. Moreover, the crab angle β_c is constant and satisfies $|\beta_c| \le \overline{\beta}_c$, where $\overline{\beta}_c < \frac{\pi}{4}$.*

Assumption 1 implies that the crab vector is contained within the set

$$Z := \{z \in \mathbb{S} : z_1 \ge 0, |z_2| \le \sin(\overline{\beta}_c)\}. \tag{6}$$

Remark 1. *Assumption 1 should not be confused with the small crab angle assumption, which assumes that the crab angle β_c is small enough such that the approximations $\cos\beta_c \approx 1$ and $\sin\beta_c \approx \beta_c$ are valid. In other words, the small crab angle assumption amounts to a control design for a model linearized around $\beta_c = 0$.*

By a path, we mean a continuous mapping $\gamma : \mathbb{R} \to \mathbb{R}^2$. Note that this object is often referred to as a curve, while a path is a curve whose domain is a compact interval. The following definition, also utilized in [8], entails the necessary regularity of the paths that we require to derive the results presented in this paper.

Definition 1. *Let $r \ge 1$. A path $\gamma : \mathbb{R} \to \mathbb{R}^2$ is $\mathcal{C}^r$ regular if*

- *it is $\mathcal{C}^r$;*
- *it holds that $\gamma'(s) \neq 0$ for all $s \in \mathbb{R}$;*
- *the arc length $\ell : \mathbb{R} \to \mathbb{R}$, defined by*

$$\ell(s) := \int_0^s |\gamma'(\eta)| \, \mathrm{d}\eta, \tag{7}$$

satisfies $\ell(\mathbb{R}) = \mathbb{R}$.

A $\mathcal{C}^r$ regular path γ is a $\mathcal{C}^r$ path with the additional property that its arc length ℓ is a $\mathcal{C}^r$ diffeomorphism from $\mathbb{R}$ to $\mathbb{R}$. Hence, the arc length reparametrization of γ, that is $s \mapsto \gamma(\ell^{-1}(s))$, is also a $\mathcal{C}^r$ regular path. If a path is $\mathcal{C}^1$, then ℓ exists and the last condition in Definition 1 is equivalent to

$$\lim_{s \to -\infty} \ell(s) = -\infty, \quad \lim_{s \to \infty} \ell(s) = \infty. \tag{8}$$

Sufficient conditions for γ to be $\mathcal{C}^r$ regular are that γ is $\mathcal{C}^r$ and that there exists $\epsilon > 0$ such that $|\gamma'(s)| \ge \epsilon$ for all $s \in \mathbb{R}$.

If a path is $\mathcal{C}^1$ regular, then we can always define a continuous tangent vector field with unit length, $\tau : \mathbb{R} \to \mathbb{S}$, by

$$\tau(s) := \frac{\gamma'(s)}{|\gamma'(s)|}. \tag{9}$$

Moreover, if γ is $\mathcal{C}^2$ regular, then τ is $\mathcal{C}^1$, and we can define a continuous signed curvature function $\kappa : \mathbb{R} \to \mathbb{R}$ by

$$\kappa(s) := \frac{\langle \tau'(s), S\tau(s) \rangle}{|\gamma'(s)|}. \tag{10}$$

If γ is parametrized by arc length, that is if $\ell(s) = s$ or equivalently $|\gamma'(s)| = 1$, then the tangent and signed curvature have the simpler expressions $\tau(s) = \gamma'(s)$ and $\kappa(s) = \langle \gamma''(s), S\gamma'(s) \rangle$, respectively.

III. MANEUVERING LINE-OF-SIGHT GUIDANCE

In this section we will present the required background material before introducing the MALOS guidance law in Section IV. Specifically, we will present the maneuvering problem and the maneuvering LOS (MLOS) algorithm, which is a proportional LOS guidance law first introduced in [11]. The MLOS algorithm does not include integral action and is designed for a unicycle model by assuming that the crab angle is zero.

We consider the control problem as a maneuvering problem [10], which consists of a geometric and a dynamic task.

Maneuvering problem:

1) **Geometric task:** Force the position of the vehicle to converge to the desired path,
$$\lim_{t\to\infty} |p(t) - \gamma(s(t))| = 0. \tag{11}$$
2) **Dynamic task:** Force the path speed to converge to the desired speed assignment:
$$\lim_{t\to\infty} |\dot{s}(t) - v_r(s(t))| = 0. \tag{12}$$

We can solve the maneuvering problem for the underactuated system (1) by employing a line-of-sight guidance law together with an appropriate update law for the path parameter s. To this end, we define the along-track and cross-track errors according to the first and second components of the vector
$$\varepsilon(p,s) := R(\tau(s))^{\mathsf{T}}(p - \gamma(s)), \tag{13}$$
respectively. The LOS guidance law will ensure that the cross-track error ε_2 tends to zero, while the update law for s will ensure that the along-track error ε_1 tends to zero. The LOS guidance law is defined by [12]
$$\bar{\zeta}(p,s) := R(z_\Delta(p,s))\tau(s), \tag{14}$$
where
$$z_\Delta(p,s) = \frac{1}{\sqrt{\Delta^2 + \varepsilon_2(p,s)^2}} \begin{pmatrix} \Delta \\ -\varepsilon_2(p,s) \end{pmatrix}, \tag{15}$$
denotes the line-of-sight vector and $\Delta > 0$ is the lookahead-distance [14]. As in [15] and [8], we note that the angle representing $\bar{\zeta}$ on the interval $(-\pi, \pi]$ is equivalent to the sum of the angles corresponding to the unit vectors $\bar{\zeta}$ and τ, mapped to the interval $(-\pi, \pi]$. Finally, the speed assignment
$$v_r(s) := \frac{U}{|\gamma'(s)|}, \tag{16}$$
ensures that $|\dot{\gamma}(s(t))| \to U$ if $\dot{s}(t) \to v_r(s(t))$.

When the effects of environmental disturbances such as wind and ocean currents are neglected, the crab angle will be zero and consequently $R(\beta) = I$. In this case, consider the update law for s given by
$$\dot{s} = e_1^{\mathsf{T}} z_\Delta(p,s) v_r(s) + \frac{\mu}{|\gamma'(s)|}\varepsilon_1(p,s), \tag{17}$$
where $\mu > 0$. The first term represents the along-track velocity, while the latter term is a so-called "gradient feedback" term [11], ensuring that the along-track error ε_1 tends to zero. The following theorem can be found in [11].

Theorem 1. *Let γ be $\mathcal{C}^1$ regular and assume that $\beta = e_1$. The maneuvering LOS (MLOS) control law given by* (14) *and* (17) *renders the set*
$$\mathcal{B} := \{(p,s) \in \mathbb{R}^3 : p = \gamma(s)\}, \tag{18}$$
UGAS for the closed-loop system
$$\begin{aligned} \dot{p} &= uR(z_\Delta(p,s))\tau(s) \\ \dot{s} &= e_1^{\mathsf{T}} z_\Delta(p,s) v_r(s) + \frac{\mu}{|\gamma'(s)|}\varepsilon_1(p,s). \end{aligned} \tag{19}$$

IV. MANEUVERING ADAPTIVE LINE-OF-SIGHT GUIDANCE

This section presents the main results of the paper. Specifically, we introduce the MALOS guidance law and prove UGAS of the origin of the resulting closed-loop system. The MALOS algorithm is a generalization of the MLOS algorithm for the case of a nonzero crab angle and includes integral action in the form of crab angle parameter estimation.

In the case of a nonzero crab angle, we propose to rotate the LOS guidance law (14) by an estimate $\hat{\beta} \in Z$ of the crab vector, i.e.
$$\zeta(p,s,\hat{\beta}) = R(\hat{\beta})^{\mathsf{T}} R(z_\Delta(p,s))\tau(s). \tag{20}$$
The update laws for $\hat{\beta}$ and s are synthesized from a Lyapunov function and are given by
$$\dot{\hat{\beta}} \in S\hat{\beta}\,\overline{\mathrm{Proj}}\left(\frac{k\varepsilon_2(p,s)\left(\Delta + \varepsilon_1(p,s)\right)}{\sqrt{\Delta^2 + \varepsilon_2(p,s)^2}}, \hat{\beta}_2, \sin(\overline{\beta}_c)\right) \tag{21}$$
$$\dot{s} = e_1^{\mathsf{T}} z_\Delta(p,s)\tilde{v}_r(s,\hat{\beta},u) + \frac{\mu}{|\gamma'(s)|}\varepsilon_1(p,s) \tag{22}$$
where $k > 0$ denotes the adaptation gain and $\tilde{v}_r : \mathbb{R} \times Z \times \mathbb{R}^2 \to \mathbb{R}$ is a modified speed assignment defined by
$$\tilde{v}_r(s,\hat{\beta},u) := \frac{u^{\mathsf{T}}\hat{\beta}}{|\gamma'(s)|}. \tag{23}$$
The first term in (22) represents the along-track velocity when $\beta \neq 0$ and reduces to the first term in (17) if $\hat{\beta} = \beta$, in other words $\tilde{v}_r(s,\beta,u) = v_r(s)$. It follows that the dynamic task is achieved if the geometric task is achieved and $\hat{\beta} \to \beta$. The set-valued $\overline{\mathrm{Proj}}$ operator utilized in (21) ensures that the estimate $\hat{\beta}$ remains within the set Z defined in (6). The operator is defined as in [16] and [8] by
$$\overline{\mathrm{Proj}}(\sigma,\varphi,a) := \left\{\varsigma\sigma : \begin{matrix} \varsigma = 1 & \text{if } \sigma \in \mathrm{T}_{[-a,a]}(\varphi) \\ \varsigma \in [0,1] & \text{if } \sigma \notin \mathrm{T}_{[-a,a]}(\varphi) \end{matrix}\right\} \tag{24}$$
where the tangent cone $\mathrm{T}_{[-a,a]} : [-a,a] \rightrightarrows \mathbb{R}$ is defined by
$$\mathrm{T}_{[-a,a]}(\varphi) := \begin{cases} [0,\infty), & \text{if } \varphi = -a \\ (-\infty,\infty), & \text{if } \varphi \in (-a,a) \\ (-\infty,0], & \text{if } \varphi = a \end{cases} \tag{25}$$

The following theorem generalizes the result in Theorem 1 to the case of a nonzero crab angle.

Theorem 2. *Let γ be $\mathcal{C}^2$ regular. If there exists $\overline{\kappa} > 0$ such that $|\kappa(s)| \leq \overline{\kappa}$ for all $s \in \mathbb{R}$, then the control law given by* (20), (21) *and* (22) *renders the set*
$$\mathcal{A} := \left\{(p,s,\hat{\beta}) \in \mathbb{R}^3 \times Z : p = \gamma(s), \hat{\beta} = \beta\right\} \tag{26}$$

UGAS for the closed-loop system

$$\dot{p} = UR(\beta)R(\hat{\beta})^{\mathsf{T}}R(\tau(s))z_\Delta(p,s) \tag{27a}$$

$$\dot{s} = e_1^{\mathsf{T}}z_\Delta(p,s)\tilde{v}_r(s,\hat{\beta},u) + \frac{\mu}{|\gamma'(s)|}\varepsilon_1(p,s) \tag{27b}$$

$$\dot{\hat{\beta}} \in S\hat{\beta}\overline{\mathrm{Proj}}\left(\frac{k\varepsilon_2(p,s)(\Delta+\varepsilon_1(p,s))}{\sqrt{\Delta^2+\varepsilon_2(p,s)^2}}, \hat{\beta}_2, \sin(\overline{\beta}_c)\right). \tag{27c}$$

Proof. We perform the change of variables $(p,\hat{\beta}) \mapsto (\varepsilon,\hat{\beta})$, where ε is defined by (13), and view $t \mapsto s(t)$ as a time-varying signal. The closed-loop system in the new coordinates is given by

$$\begin{aligned}\dot{\varepsilon} = &-\kappa(s(t))\lambda(\varepsilon,\hat{\beta})S\varepsilon + UR(\beta)R(\hat{\beta})^{\mathsf{T}}z_\Delta(\varepsilon)\\ &- e_1\lambda(\varepsilon,\hat{\beta})\end{aligned} \tag{28a}$$

$$\dot{\hat{\beta}} \in S\hat{\beta}\overline{\mathrm{Proj}}\left(\frac{k\varepsilon_2\,(\Delta+\varepsilon_1)}{\sqrt{\Delta^2+\varepsilon_2^2}}, \hat{\beta}_2, \sin(\overline{\beta}_c)\right), \tag{28b}$$

and evolves in the state space $\mathbb{R}^2 \times Z$. The function $\lambda : \mathbb{R}^2 \times Z \to \mathbb{R}$ is defined by

$$\lambda(\varepsilon,\hat{\beta}) := \frac{\Delta(u_1\hat{\beta}_1 + u_2\hat{\beta}_2)}{\sqrt{\Delta^2+\varepsilon_2^2}} + \mu\varepsilon_1. \tag{29}$$

Our aim is to render the compact set

$$\mathcal{A}_1 := \{(\varepsilon,\hat{\beta}) \in \mathbb{R}^2 \times Z : \varepsilon = 0, \hat{\beta} = \beta)\} \tag{30}$$

UGAS for (28). To this end, we define the continuously differentiable function $V_1 : \mathbb{R}^2 \times Z \to \mathbb{R}$ by

$$V_1(\varepsilon,\hat{\beta}) := \frac{1}{2}|\varepsilon|^2 + \frac{U}{k}(1-\beta^{\mathsf{T}}\hat{\beta}), \tag{31}$$

which is positive definite relative to $\mathcal{A}_1$ and proper since $\varepsilon \mapsto \frac{1}{2}|\varepsilon|^2$ is radially unbounded, Z is compact and $\hat{\beta} \mapsto \frac{U}{k}(1-\beta^{\mathsf{T}}\hat{\beta})$ is continuous. It can be shown that

$$\begin{aligned}\dot{V}_1(\varepsilon,\hat{\beta},\xi) = &-\frac{U\,\beta^{\mathsf{T}}\hat{\beta}}{\sqrt{\Delta^2+\varepsilon_2^2}}\varepsilon_2^2 - \mu\,\varepsilon_1^2\\ &+ \beta^{\mathsf{T}}S\hat{\beta}\left(\frac{\varepsilon_2(\Delta+\varepsilon_1)}{\sqrt{\Delta^2+\varepsilon_2^2}} - \frac{\xi}{k}\right),\end{aligned} \tag{32}$$

where ξ is a placeholder for the crab estimate update law,

$$\xi \in \overline{\mathrm{Proj}}\left(\frac{k\varepsilon_2\,(\Delta+\varepsilon_1)}{\sqrt{\Delta^2+\varepsilon_2^2}}, \hat{\beta}_2, \sin(\overline{\beta}_c)\right). \tag{33}$$

It is clear that the last term in (32) vanishes identically if the integrator is not saturated. If the integrator is saturated, for instance when $\hat{\beta}_2 = \sin\overline{\beta}_c$ and $\varepsilon_2(\Delta+\varepsilon_1) > 0$, then $\beta^{\mathsf{T}}S\hat{\beta} = -\sin(\overline{\beta}_c)\beta_1 + \cos(\overline{\beta}_c)\beta_2$, which is nonpositive for all $\beta \in Z$. Since the term in parentheses in (32) is nonnegative in this case, the entire last term in (32) is nonpositive. A similar argument holds in the other case where the integrator saturates, that is when $\hat{\beta}_2 = -\sin\overline{\beta}_c$ and $\varepsilon_2(\Delta+\varepsilon_1) < 0$. Hence, defining the continuous function $Y_1 : \mathbb{R}^2 \times Z \to \mathbb{R}$ by

$$Y_1(\varepsilon,\hat{\beta}) := -\frac{U\cos(2\overline{\beta}_c)}{\sqrt{\Delta^2+\varepsilon_2^2}}\varepsilon_2^2 - \mu\,\varepsilon_1^2, \tag{34}$$

it holds that $\dot{V}_1(\varepsilon,\hat{\beta},\xi) \le Y_1(\varepsilon,\hat{\beta})$ for all $(\varepsilon,\hat{\beta}) \in \mathbb{R}^2 \times Z$ and all ξ selected according to (33). It follows that $\mathcal{A}_1$ is UGS for (28). Now, we consider a second continuously differentiable function $V_2 : \mathbb{R}^2 \times Z \to \mathbb{R}$ defined by

$$V_2(\varepsilon,\hat{\beta}) := -\varepsilon^{\mathsf{T}}R(\hat{\beta})^{\mathsf{T}}\beta. \tag{35}$$

From (28), we find that

$$\begin{aligned}\dot{V}_2(\varepsilon,\hat{\beta},\xi,t) = &-\kappa(s(t))\lambda(\varepsilon,\hat{\beta})\varepsilon^{\mathsf{T}}SR(\hat{\beta})^{\mathsf{T}}\beta\\ &- Uz_\Delta(\varepsilon)^{\mathsf{T}}e_1 + \lambda(\varepsilon,\hat{\beta})e_1^{\mathsf{T}}R(\hat{\beta})^{\mathsf{T}}\beta\\ &+ \xi\varepsilon^{\mathsf{T}}SR(\hat{\beta})^{\mathsf{T}}\beta.\end{aligned} \tag{36}$$

We now define the continuous function $Y_2 : \mathbb{R}^2 \times Z \to \mathbb{R}$ by

$$\begin{aligned}Y_2(\varepsilon,\hat{\beta}) := &\;\overline{\kappa}|\lambda(\varepsilon,\hat{\beta})||\varepsilon| - Uz_\Delta(\varepsilon)^{\mathsf{T}}e_1\\ &+ \lambda(\varepsilon,\hat{\beta})\beta^{\mathsf{T}}\hat{\beta} + \frac{k|\varepsilon||\varepsilon_2||\Delta+\varepsilon_1|}{\sqrt{\Delta^2+\varepsilon_2^2}}.\end{aligned} \tag{37}$$

It is then straightforward to show that $\dot{V}_2(\varepsilon,\hat{\beta},\xi,t) \le Y_2(\varepsilon,\hat{\beta})$ for all $(\varepsilon,\hat{\beta}) \in \mathbb{R}^2 \times Z$, all t, and all ξ selected according to (33). Since $Y_1^{-1}(0) = \{(\varepsilon,\hat{\beta}) \in \mathbb{R}^2 \times Z : \varepsilon = 0\}$,

$$\begin{aligned}Y_2(0,\hat{\beta}) &= -U + \lambda(0,\hat{\beta})\beta^{\mathsf{T}}\hat{\beta}\\ &= -U(1-(\beta^{\mathsf{T}}\hat{\beta})^2) \le 0,\end{aligned} \tag{38}$$

and $Y_1^{-1}(0) \cap Y_2^{-1}(0) = \mathcal{A}_1$, we have that $\mathcal{A}_1$ is UGAS for (28) by [17, Theorem 4.1]. UGAS of the compact set $\mathcal{A}_1$ for (28) can be identified with UGAS of the noncompact set $\mathcal{A}$ for (27). Indeed, UGAS of $\mathcal{A}_1$ implies that there exists $\alpha \in \mathcal{KL}$ such that every solution $t \mapsto \phi_1(t)$ to (28) satisfies $|\phi_1(t)|_{\mathcal{A}_1} \le \alpha(|\phi_1(0)|_{\mathcal{A}_1}, t)$ for all $t \in \operatorname{dom}\phi_1$. Therefore, since

$$\begin{aligned}|(\varepsilon,\hat{\beta})|_{\mathcal{A}_1} &= \sqrt{|\varepsilon|^2 + |\hat{\beta}-\beta|^2}\\ &= \sqrt{|p-\gamma(s)|^2 + |\hat{\beta}-\beta|^2}\\ &= |(p,s,\hat{\beta})|_{\mathcal{A}},\end{aligned} \tag{39}$$

it follows that every solution $t \mapsto \phi(t)$ to (27) satisfies $|\phi(t)|_{\mathcal{A}} \le \alpha(|\phi(0)|_{\mathcal{A}}, t)$ for all $t \in \operatorname{dom}\phi$. Hence, $\mathcal{A}$ is UGAS for (27). □

In a non-maneuvering setting such as [8], an alternative update law to (27b) is utilized which ensures that the along-track error ε_1 is equal to zero at all times. If ε_1 could be maintained at zero, our crab vector update law (27c) would be equivalent to the one adopted in the ALOS guidance law [7], except for the fact that we use the set-valued projection operator instead of the locally Lipschitz projection operator [18, Appendix E]. However, maintaining the along-track error ε_1 at zero through selection of the path parameter can in general only be achieved locally, if we demand that $t \mapsto s(t)$ is continuous. To illustrate this fact, imagine that a marine vehicle is initialized at the center of a circular path. At this particular position, every choice of $s \in \mathbb{R}$ ensures that ε_1 is zero. If the position of the vehicle now is perturbed slightly in any direction, there is only one valid choice of path parameter (up to the periodicity of the path). Thus, for almost all initial choices $s(t_0)$ of the path parameter, $t \mapsto s(t)$

must be discontinuous at $t = t_0$ when the vehicle position is perturbed if the along-track error is to be maintained at zero. A discontinuity in s at t_0 implies that the unit tangent vector $t \mapsto \tau(s(t))$ is discontinuous at t_0 and hence that the LOS guidance law control signal is discontinuous at t_0. On the other hand, the MALOS algorithm ensures that $t \mapsto s(t)$ is continuously differentiable and guarantees global asymptotic path following without requiring that the along-track error ε_1 is identically equal to zero.

Remark 2. *The crab vector estimate update law* (21) *can be cast in terms of an equivalent crab angle estimate update law as*

$$\begin{aligned}\dot{\hat{\beta}}_c &\in \operatorname{Proj}\left(\frac{k\varepsilon_2(p,s)\,(\Delta+\varepsilon_1(p,s))}{\sqrt{\Delta^2+\varepsilon_2(p,s)^2}}, \hat{\beta}_c, \overline{\beta}_c\right), \\ \hat{\beta} &= (\cos\hat{\beta}_c, \sin\hat{\beta}_c).\end{aligned} \tag{40}$$

The alternative update law (40) *can be implemented as a standard saturated scalar integrator. In particular, if an explicit Euler discretization is utilized,*

$$\hat{\beta}_c^+ = \operatorname{sat}\left(\hat{\beta}_c + \frac{kT\varepsilon_2(p,s)\,(\Delta+\varepsilon_1(p,s))}{\sqrt{\Delta^2+\varepsilon_2(p,s)^2}}\right) \tag{41}$$

where $\operatorname{sat} x := \min(\overline{\beta}_c, \max(-\overline{\beta}_c, x))$ *and* $T > 0$ *is the discretization step size. Hence, despite seeming more complicated at first glance, utilization of the set-valued projection operator in fact simplifies the implementation compared to the locally Lipschitz projection operator.*

V. Case Study

In this section, we present a simulation case study that demonstrates the efficacy of the MALOS guidance law for two extreme but realistic scenarios. We utilize a 6-degree-of-freedom dynamic model of a Kongsberg Remus 100 AUV with model parameters acquired from [19]. The output of the MALOS algorithm (20) serves as the setpoint to a lower-level proportional-integral-derivative (PID) heading autopilot. The forward speed is controlled indirectly by setting the propeller revolution to 550 revolutions per minute, corresponding to a forward velocity of approximately $0.9\,\mathrm{m/s}$ in calm waters. In all of the simulations we consider an ocean current coming from the south with a speed of $0.2\,\mathrm{m/s}$. Moreover, we set the parameters in the control law given by (20)–(22) as $k = 0.015$, $\Delta = 10$, $\mu = 5$ and $\overline{\beta}_c = 13°$.

The first scenario considers west-east straight-line path following, and is meant to test two important aspects of the MALOS guidance law:

- The transient performance, and in particular the degree of overshoot, when the vehicle is initialized far away from the path.
- The estimation of the crab angle when conditions approach a steady state.

The second scenario investigates path following for a lemniscate, a $\mathcal{C}^\infty$ regular path defined by

$$\gamma(s) := \begin{pmatrix} R_1 \frac{\sqrt{2}\sin(2s)}{1+\sin(s)^2} \\ R_2 \frac{\cos s}{1+\sin(s)^2}\end{pmatrix}, \tag{42}$$

where $R_1 = 20$ and $R_2 = 40$. This scenario is meant to test the following important aspects of the MALOS guidance law:

- The overall performance of the guidance law in a highly dynamic path following scenario.
- The estimation of the crab angle when steady state conditions never arise.

For each scenario, we compare the north-east trajectories obtained by employing MALOS and MLOS, that is, with and without integral action. Furthermore, we compare the crab angle estimates from MALOS with the true crab angle, and the desired heading from MALOS with the yaw angle from the 6-degree-of-freedom simulation model.

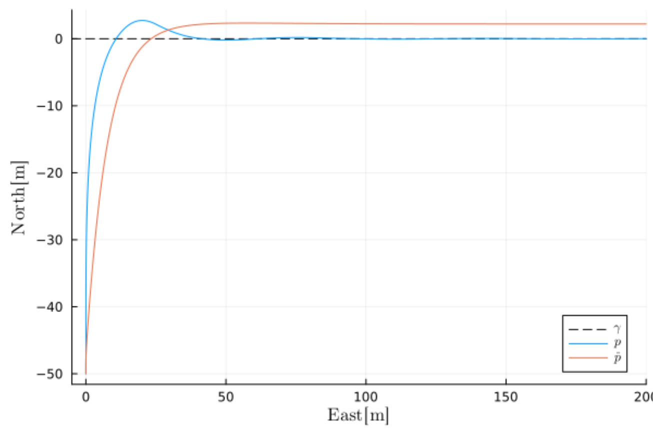

Fig. 1. The reference path γ and the north-east trajectories p and $\tilde{p}$ obtained by employing the MALOS (blue) and MLOS (red) control laws given by (20)–(22) and (14) and (17), respectively.

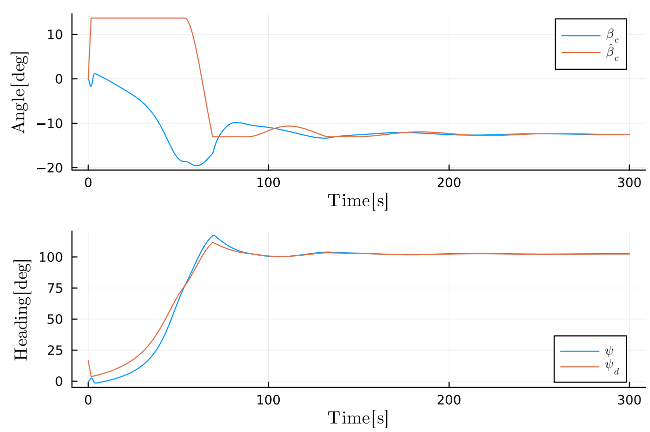

Fig. 2. The crab angle β_c and the estimated crab angle $\hat{\beta}_c = \operatorname{atan2}(\hat{\beta}_2, \hat{\beta}_1)$, and the heading ψ and the desired heading $\psi_d = \operatorname{atan2}(\zeta_2, \zeta_1)$.

Simulation results for the first scenario are presented in Fig. 1 and Fig. 2. Since the north position is initialized 50 meters away from the path, the integral state $\hat{\beta}$ saturates quickly at $t \approx 2\,\mathrm{s}$, as seen in Fig. 2. This helps minimize the resulting overshoot when we approach the path. Indeed, Fig. 1 shows that the overshoot is only marginally larger than the steady state error of the MLOS algorithm. Furthermore, we note that the crab angle estimate $\hat{\beta}_c$ approaches the actual crab angle β when we approach steady state conditions.

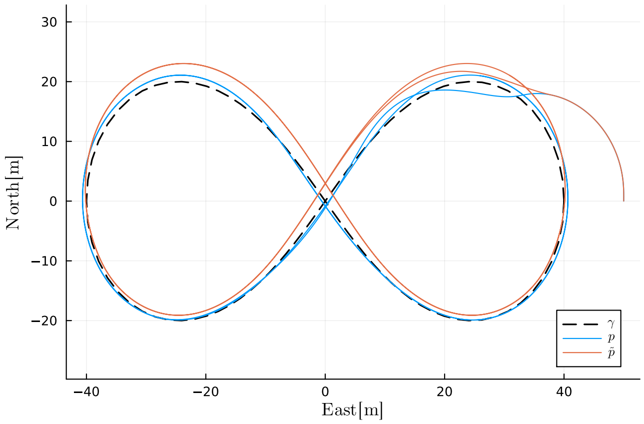

Fig. 3. The reference path γ and the north-east trajectories p and $\tilde{p}$ obtained by employing the MALOS (blue) and MLOS (red) control laws given by (20)–(22) and (14) and (17), respectively.

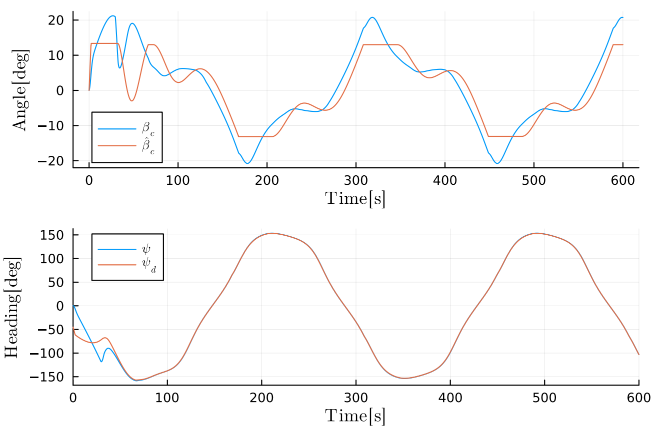

Fig. 4. The crab angle β_c and the estimated crab angle $\hat{\beta}_c = \text{atan2}(\hat{\beta}_2, \hat{\beta}_1)$, and the heading ψ and the desired heading $\psi_d = \text{atan2}(\zeta_2, \zeta_1)$.

Simulation results for the second scenario are presented in Fig. 3 and Fig. 4. This is a demanding scenario in which the crab angle β_c is never constant, and hence the conditions of Assumption 1 are never satisfied. Nevertheless, by comparing the north-east trajectories obtained by employing the MALOS and MLOS algorithms in Fig. 3, it is clear that the integral action in the MALOS algorithm results in a trajectory that is closer to the desired path.

VI. Conclusions

This paper has introduced the maneuvering adaptive line-of-sight (MALOS) guidance law. MALOS ensures global asymptotic curved path following and crab angle estimation for a class of underactuated vehicles in the presence of an unknown crab angle. The stability results are truly global since the path parameter dynamics are unconstrained and included in the stability proof. This is in contrast to state of the art ILOS and ALOS guidance algorithms which abstract the path parameter dynamics away by assuming that the path parameter can be selected such that the along-track error is identically zero.

References

[1] E. Børhaug, A. Pavlov, and K. Y. Pettersen, “Integral LOS control for path following of underactuated marine surface vessels in the presence of constant ocean currents,” in *Proc. 47th IEEE Conference on Decision and Control*. Cancun, Mexico: IEEE, 2008, pp. 4984–4991.

[2] W. Caharija, K. Y. Pettersen, M. Bibuli, P. Calado, E. Zereik, J. Braga, J. T. Gravdahl, A. J. Sørensen, M. Milovanovic, and G. Bruzzone, “Integral Line-of-Sight Guidance and Control of Underactuated Marine Vehicles: Theory, Simulations, and Experiments,” *IEEE Transactions on Control Systems Technology*, vol. 24, no. 5, pp. 1623–1642, Sep. 2016.

[3] E. Kelasidi, P. Liljebäck, K. Y. Pettersen, and J. T. Gravdahl, “Integral line-of-sight guidance for path following control of underwater snake robots: Theory and experiments,” *IEEE Transactions on Robotics*, vol. 33, no. 3, pp. 610–628, 2017.

[4] T. I. Fossen, K. Y. Pettersen, and R. Galeazzi, “Line-of-sight path following for dubins paths with adaptive sideslip compensation of drift forces,” *IEEE Transactions on Control Systems Technology*, vol. 23, no. 2, pp. 820–827, Mar. 2015.

[5] L. Liu, D. Wang, and Z. Peng, “ESO-based line-of-sight guidance law for path following of underactuated marine surface vehicles with exact sideslip compensation,” *IEEE Journal of Oceanic Engineering*, vol. 42, no. 2, pp. 477–487, Apr. 2017.

[6] T. I. Fossen, “An adaptive line-of-sight (ALOS) guidance law for path following of aircraft and marine craft,” *IEEE Transactions on Control Systems Technology*, pp. 1–8, 2023.

[7] T. I. Fossen and A. P. Aguiar, “A uniform semiglobal exponential stable adaptive line-of-sight (ALOS) guidance law for 3-D path following,” *Automatica*, vol. 163, p. 111556, May 2024.

[8] H. M. Schmidt-Didlaukies, E. A. Basso, and K. Y. Pettersen, “Input-to-state stable integral line-of-sight guidance for curved paths with anti-windup guarantees,” *IEEE Control Systems Letters*, vol. 8, pp. 730–735, 2024.

[9] R. Skjetne, T. I. Fossen, and P. V. Kokotović, “Robust output maneuvering for a class of nonlinear systems,” *Automatica*, 2004.

[10] R. Skjetne, “The maneuvering problem,” PhD Thesis, Norwegian University of Science and Technology, 2005.

[11] R. Skjetne, U. Jørgensen, and A. R. Teel, “Line-of-sight path-following along regularly parametrized curves solved as a generic maneuvering problem,” in *Proc. IEEE Conference on Decision and Control and European Control Conference*, Orlando, FL, USA, Dec. 2011.

[12] M. Marley, R. Skjetne, E. A. Basso, and A. R. Teel, “Maneuvering with safety guarantees using control barrier functions,” *IFAC-PapersOnLine*, vol. 54, no. 16, pp. 370–377, 2021.

[13] M. Marley, R. Skjetne, and A. R. Teel, “A kinematic hybrid feedback controller on the unit circle suitable for orientation control of ships,” in *Proc. 59th Conf. on Decision and Control*, Jeju Island, Republic of Korea, 2020.

[14] T. I. Fossen, *Handbook of Marine Craft Hydrodynamics and Motion Control*, 2nd ed. Wiley, 2020.

[15] E. L. Foseid, E. A. Basso, H. M. Schmidt-Didlaukies, M. Marley, K. Y. Pettersen, and J. T. Gravdahl, “Learning optimal guidance schemes with safety guarantees for underactuated marine vehicles,” in *Proc. 15th IFAC Conference on Control Applications in Marine Systems, Robotics and Vehicles*, Blacksburg, VA, USA, Sep. 2024.

[16] E. A. Basso, H. M. Schmidt-Didlaukies, and K. Y. Pettersen, “Global asymptotic position and heading tracking for multirotors using tuning function-based adaptive hybrid feedback,” *IEEE Control Systems Letters*, vol. 7, pp. 295–300, 2023.

[17] R. Sanfelice and A. Teel, “Asymptotic stability in hybrid systems via nested matrosov functions,” *IEEE Transactions on Automatic Control*, vol. 54, no. 7, pp. 1569–1574, Jul. 2009.

[18] M. Krstic, P. V. Kokotovic, and I. Kanellakopoulos, *Nonlinear and Adaptive Control Design*. John Wiley & Sons, 1995.

[19] T. I. Fossen and T. Perez, “Marine Systems Simulator (MSS),” 2004. [Online]. Available: https://github.com/cybergalactic/MSS